Journal of Microbiological Methods 194 (2022) 106436

Contents lists available at ScienceDirect

Journal of Microbiological Methods

journal homepage: www.elsevier.com/locate/jmicmeth

Determination of streptomycin and doxycycline using LC/MS towards an effective treatment against an experimental *Brucella abortus* infection in mice

Eugenia Sancho [a], Fabio Granados-Chinchilla [b,*], Elías Barquero-Calvo [a]

[a] Tropical Diseases Research Program, School of Veterinary Medicine, 86-3000, National University, Heredia, Costa Rica
[b] Centro Nacional de Ciencia y Tecnología de Alimentos, 11501-2060, Sede Rodrigo Facio, Universidad de Costa Rica, Costa Rica

ARTICLE INFO

Keywords:
LC/MS
Streptomycin
Doxycycline
Brucellosis therapy
Murine animal model
Internal organs
Plasma

ABSTRACT

Herein we described a versatile liquid chromatographic method for detection and quantification of the total levels of two antimicrobials [i.e., streptomycin (STM) and doxycycline (DOX)], in mice plasma and selected tissues, with the aid of a single quadrupole as a detection method. The method included a few sample preparation steps, including freeze-drying and *in situ* triphasic solvent-assisted defatting, precipitation, and extraction, allowing easy and fast tissue sample processing and avoiding analyte loss. Using a murine model, we demonstrated that mass spectrometry detects simultaneously and with high specificity two of the most widespread antimicrobials used against Brucellosis. An accurate [recoveries varied from 75.23 (bone marrow) to 101.33% (liver)] and sensitive (LoD in the ng g^{-1} range) method to assess STM and DOX in murine tissue, including subtherapeutic and therapeutic doses of the antimicrobials, was achieved. This validated method can be successfully used to monitor the depletion of STM and DOX in several mice tissues and plasma during metabolism after administration.

1. Introduction

Brucellosis (a disease caused by bacteria from the genus *Brucella*) affects wildlife, domestic animals, and humans (Whatmore and Foster, 2021). This infection is one of the most common bacterial zoonotic diseases worldwide, causing approximately 500,000 cases identified annually worldwide (Harrison and Posada, 2018; Pappas et al., 2006). Chronic bacterial infections such as Brucellosis usually require prolonged antibiotic treatments (Solera, 2010).

Various therapeutic protocols have been proposed for treating Brucellosis (Solera, 2010). The most common treatments include tetracyclines (in combination with an aminoglycoside), rifampicin, trimethoprim-sulfamethoxazole, or quinolones (Abo El-Ela et al., 2020; Solera, 2010).

The combination of DOX with STM is accepted to be the most effective regimen in Brucellosis. Other treatment options are associated with worse outcomes (Alp et al., 2006; Alavi and Alavi, 2013). DOX is a semi-synthetic derivative of tetracycline and is the result of transferring the C6 hydroxyl group of tetracycline to C5 (Vardanyan and Hruby, 2006). On the other hand, STM is a pseudotrisaccharide having a monosubstituted aminocyclitol to which a disaccharide is attached (Kirst and Allen, 2007). Both antibiotics inhibit bacterial protein synthesis by binding to the 16S rRNA of the 30S bacterial ribosome subunit, thus preventing accommodation of incoming aminoacyl-tRNAs at the acceptor site (A-site) and a broad spectrum of antibacterial activity (i.e., effective for most Gram-negative and a few Gram-positive bacteria) (Krause et al., 2016; Markley and Wencewicz, 2018).

Even though there are seemingly appropriate antibiotics for treating Brucellosis, there is a high incidence of post-treatment relapses that ranges from 5% to 30% (Solera, 2010). Furthermore, these relapses occur even if *Brucella* isolates (cultivated from these relapses) remain susceptible to the antibiotics initially used (Solera, 2010).

There is an important gap in the literature regarding the study of relapses in Brucellosis. This gap is due in part to the absence of validated animal models. These animal models are essential to evaluate the doses, the antibiotic type, the combinations, and the regimens to assess the effectiveness of the treatment. In addition, due to the ease of handling and low maintenance costs, the mouse has been widely used to study Brucellosis (Grilló et al., 2012; Silva et al., 2011).

One of the critical questions in the study of Brucellosis relapses is

* Corresponding author at: Centro Nacional de Ciencia y Tecnología de Alimentos, 11501-2060, Sede Rodrigo Facio, Universidad de Costa Rica, Costa Rica.
E-mail address: fabio.granados@ucr.ac.cr (F. Granados-Chinchilla).

https://doi.org/10.1016/j.mimet.2022.106436
Received 10 January 2022; Received in revised form 22 February 2022; Accepted 22 February 2022
Available online 25 February 2022

whether the antibiotics reach the proper therapeutic concentrations at the sites of infection. Therefore, the accurate quantification of antibiotics is critical to evaluate the effective dose-response of antibiotic regimens and eventually study the relapses.

From the methodological standpoint, examples of STM analysis in tissue are few [e.g., agar diffusion (Mitchison and Spicer, 1949), spectrophotometric (Jelinek and Boxer, 1948; Boxer and Jelinek, 1947), LC-fluorescence (Gerhardt et al., 1994; Okayama et al., 1988), radioimmunoassay (Araby et al., 2020)] and unlike DOX it is usually not included in multi-analyte methods. There are, however, some other examples where LC-MS has been used to assess STM [e.g., milk (Hormazábal and Østensvik, 2009), honey (Bohm et al., 2012), and fruit (Do et al., 2015)]. Other members of the aminoglycoside family have been more widely studied, such as kanamycin (Zhang et al., 2019).

On the other hand, the most recent DOX determination in plasma or tissue relies on liquid chromatography (LC) (Chaitanya Krishna et al., 2012; Gadja et al., 2014; Mestorino et al., 2018; Selvadural et al., 2010; Xu et al., 2019; Xu et al., 2021). In tissues, DOX has the advantage that as an antibiotic of husbandry, veterinary, and even clinical application (Granados-Chinchilla and Rodríguez, 2017), it is usually found with other members of the tetracyclines in multiclass antibiotic screening methods (Giusepponi et al., 2019).

Of late, the concentration of DOX within tissues following treatment for *Yersinia pseudotuberculosis* and *Mycobacterium tuberculosis* has been reported using a fluorescent transcriptional reporter (Gengerbacher et al., 2020; Ramirez Raneses et al., 2020). However, in the past, LC has been used to monitor the depletion of antibiotics (Cazorla-Reyes et al., 2014; Cooper et al., 2005; Mestorino et al., 2018; Xu et al., 2019).

Given that no method focuses on both STM and DOX in murine models, we developed a versatile liquid chromatographic method for detection and quantification of the total levels of these two antimicrobials in mice plasma and selected tissues (i.e., spleen, liver, kidney, bone marrow), with the aid of a single quadrupole as a detection method. Finally, we performed a preliminary depletion test and monitored the remaining levels of these antibiotics in mice tissue and plasma to demonstrate if antimicrobial classes, during therapy, indeed reach target organs.

2. Materials and methods

2.1. Reagents

STM (sesquisulfate hydrate, VETRANAL®, catalog number 46754) and DOX (hyclate, VETRANAL®, catalog number 33429) analytical standards were purchased from Merck Millipore/Sigma-Aldrich (St. Louis, MO, USA). LC grade acetonitrile (ACN, catalog number 100029, LiChrosolv®), methanol (MeOH, catalog number 106035, LiChrosolv®), ammonium acetate, (catalog number Supelco, 101116, EMSURE® ACS, Reag. Ph Eur), ethanol (catalog number 02870, ACS reagent), sodium chloride (catalog number S9888, ACS reagent), and formic acid (FA, catalog number 100241, 98–100%, EMSURE® ACS, Reag. Ph Eur) were acquired from Merck Millipore (Merck KGaA, Darmstadt, Germany). Isoflurane was obtained from Abbot Laboratories (IsoFlo® 100 g/100 g, inhalation vapor, liquid, Chicago, IL, USA). Ultrapure water [type I, 0.055 μS cm^{-1} at 25 °C, 5 μg L^{-1} TOC] was obtained using an A10 Milli-Q Advantage system and an Elix 35 system (EMD Millipore Burlington, MA, USA). Chromatographic quality nitrogen was generated with a PEAK Scientific generator (NM32LA, Inchinnan, United Kingdom).

2.2. Mice selection and antibiotic administration

CD1® IGS strain mice (Charles River Laboratories, Wilmington, MA, USA) were used for experimentation and kept in the School of Veterinary Medicine vivarium of the National University. All animals were kept in cages with food and water *ad libitum* under biosecurity containment conditions. STM and DOX in mice were monitored at 12 h after administration at three different concentrations each (i.e., 40, 20, and 10 mg kg^{-1} and 200, 100, 50 mg kg^{-1}, respectively). At each point, mice were sacrificed to make measurements of antibiotics in the selected tissues.

2.3. Organ harvesting and plasma withdrawal

Sedation with isoflurane was performed previously in blood collection tubes with EDTA (from the orbital sinus) following previous protocols (ILAR, 2011). The spleen was obtained immediately after sacrifice using a previously described procedure (Barquero-Calvo et al., 2013). Briefly, the mouse was placed in a dorsal position supported by the extremities. Then, the mouse body was sprayed with ethanol (70 mL/100 mL). Next, a small cut was made (with a surgical scalpel blade) in the skin below the lower belly. Then, the abdominal cavity was opened exposing the spleen (located in the mouse's left upper abdominal quadrant). The same procedure was carried out to extract the liver and kidney.

The bone marrow was also obtained immediately after sacrifice using a previously described method (Gutierrez-Jiménez et al., 2018). Briefly, the procedure included an incision in each hind leg with sterile shears, and the skin was removed and pulled down to expose the muscles. Once the skin was removed, the hind leg was cut just above the hip joint with dissecting scissors, ensuring that the epiphysis remained intact without exposing its contents. After the hind leg was removed, an incision was made just above the claws to remove the underside of the hind leg and remove excess tissue with sterile forceps and scissors, keeping the bone ends intact. Intact bones were soaked in saline solution (0.85 g/100 mL). Subsequently, the remaining excess tissue was cleaned with sterile gauze. Next, the ends of the bones were cut and placed in microcentrifuge tubes. These tubes were centrifuged at 500 ×*g* for 3 min to extract the entire marrow content of the bones.

2.4. Antimicrobial extraction from sample

After sacrificing and extracting the organs, they were freeze-dried for 24 h (Labconco™ FreeZone™ 4.5 L Benchtop Freeze Dry Systems, Kansas City, MO, USA). Then, all the organs were manually macerated and weighed. Treated tissues were grouped in 2 mL conical tubes by weight as follows: 90, 90, and 11.8 mg for liver, spleen, and bone marrow, respectively. In the case of plasma, a 50 μL aliquot was used for processing. The spleen, liver, and bone marrow samples were processed using 200 μL of ammonium acetate buffer (1 mmol mL^{-1}, pH 5.0), 150 μL of ACN, and 150 μL of MeOH. The plasma samples were treated with 200 μL of buffer, 125 μL of ACN, and 125 μL MeOH, in a total volume of 500 μL.

The microtubes were centrifuged at 12000 ×*g* (Espresso, Thermo Scientific™). After that, the supernatant was recovered using a syringe filter (hydrophobic PTFE membrane, 0.45 μm, Acrodisc®, PALL®, NY, USA) and transferred to a conical glass 350 μL insert and 2 mL HPLC vial (Agilent Technologies, Santa Clara, CA, USA) for injection.

2.5. Chromatographic conditions

All assays were performed using an Agilent Technologies LC/MS system equipped with a 1260 infinity quaternary pump (61311C), column compartment (G1316A), automatic liquid sampler modules (ALS, G7129A), and a 6120-single quadrupole mass spectrometer with electrospray ionization ion source (ESI, Agilent Technologies, Santa Clara, CA, USA). Gradient elution was used to separate all the compounds. The solvent gradient was optimized using ACN (solvent A) and water (solvent C), both acidified with FA (0.1 mL/100 mL). Solvent proportions were set as follows: at 0 min 95% C, at 20 min 35% A and 65% C, at 25 min, at 25 min 95% C and finally at 35 min 95% C, obtaining a complete chromatographic separation for the two antibiotics. The flow rate was kept constant at 1.2 mL min^{-1}. Injection volume for all samples was held

at 20 μL. The column compartment was held at a temperature of 20.0 ± 0.8 °C. A reverse-phase chromatographic column was used to achieve the analytical separation (Eclipse Plus C_{18}, 4.6 ID × 100 mm, 3.5 μm, Agilent Technologies, PN 959961–902).

2.6. MS detection system conditions

The fragmentor was initially cycled to assess the voltage (from 20 to 300 V) that rendered the highest sensitivity for the compounds, omitting column interaction. Afterward, total ion chromatographs (TIC) allowed us to obtain the MS spectra for each compound (scan mode using a mass range and detector gain set to 50–750 *m/z*, and 10.00, respectively). Drying gas, nebulizer pressure, drying gas temperature, and capillary voltage was set, respectively, to 12.0 L min^{-1}, 50 psi, 350 °C, 4000 V for positive ion mode electrospray ionization (ESI^+). Selected Ion Monitoring (SIM) mode was set to a peak width and cycle time of 0.05 min, and 0.30 s $cycle^{-1}$, respectively.

3. Results and discussion

3.1. Sample extraction

The organic portion of the extraction solvent ensured the solubility of DOX (see below). Meanwhile, ACN and MeOH are also widely used to provide protein and lipid-free supernatants from biological samples (Hušek et al., 2012). On the other hand, the function of the ammonium acetate buffer [a common extraction buffer for antibiotics in tissue (Samanidou et al., 2016)] is twofold. First, it aids in the solubility of the DOX using acid-base behavior and serves as an aqueous vehicle for the water-soluble STM (see below). For example, DOX has three ionizable groups pK_a 3.4, 7.7 (conjugated phenolic enone system), and 9.7 (tertiary amine) (Mojica et al., 2014). At pH 5.0, only the trione-conjugated system (which is acidic in nature) will be protonated. Meanwhile, STM ionizable groups will be deprotonated as their pK_a values range from 6.7 to 8.9 (Alkhzem et al., 2020). Moreover, similarly to FA used in the mobile phase, the acetate ion facilitates the molecule fragmentation (Mallet et al., 2004) due to its degradation in the ion source.

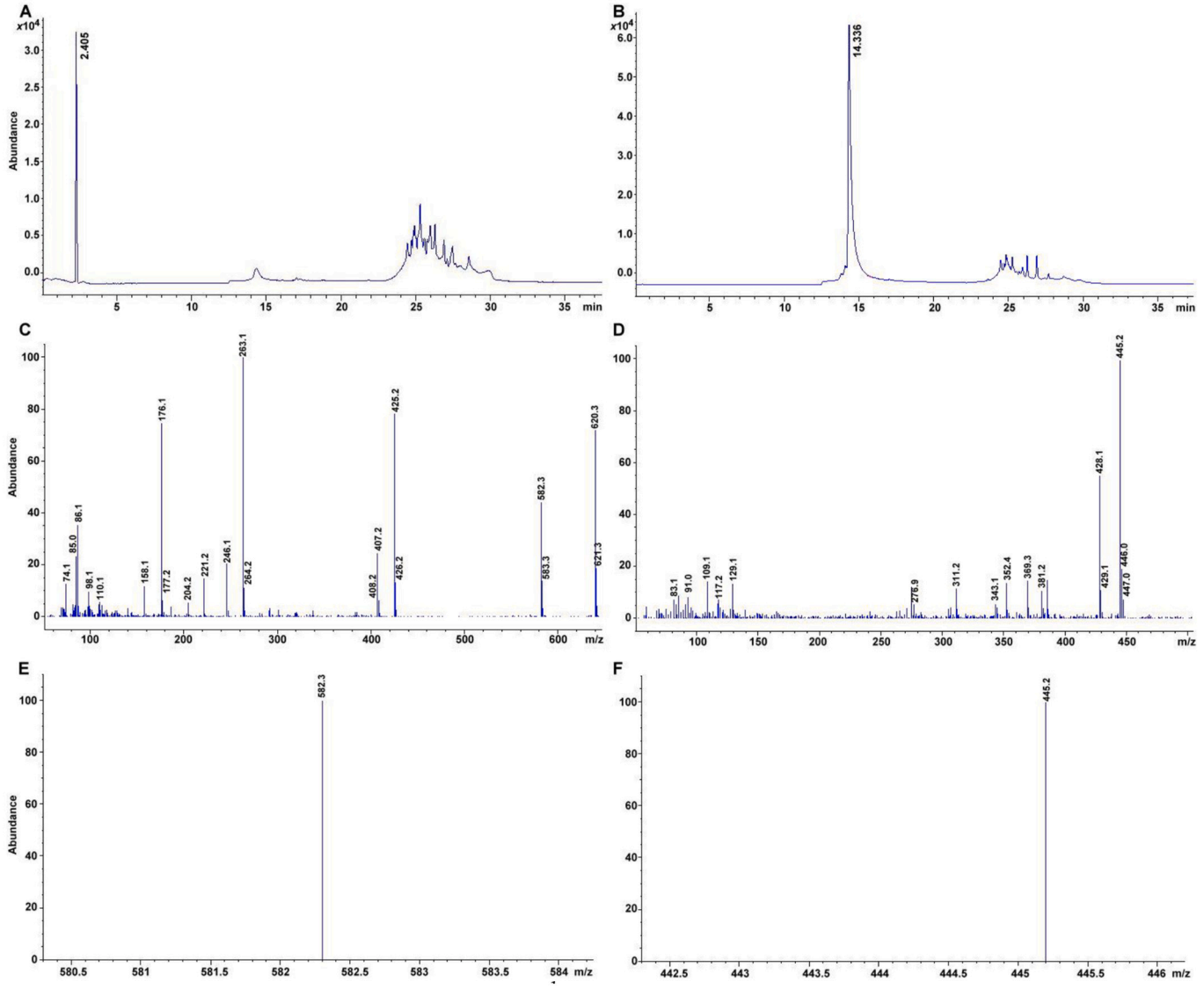

Fig. 1. SIM chromatogram for 10 μg mL^{-1} A. STM and B. DOX. Mass spectra from a total ion chromatogram (TIC) for 100 μg mL^{-1} solutions of C. STM and D. DOX. SIM for the molecular ion for 10 μg mL^{-1} solutions of E. STM and F. DOX.

3.2. Quantitative chromatographic separation of analytes

The separation considered the structural intricacies of each compound. For example, STM is highly water-soluble, whereas DOX is soluble in MeOH and sparingly in ACN. Then, under these conditions, STM eluted very early during the chromatographic run, while DOX eluted later on as the organic solvents started to gain relevance in the gradient (Fig. 1A, B). For example, under our solvent system, when DOX was eluted (R_tR ca. 14 min), only 45.5% of the solvent composition was acidified water (Fig. 1B). Accordingly, the solubility of STM in water, and methanol, at ca. 301.15 K, is calculated at $>>$ 20 and 0.85 mg mL^{-1} (Ujváry, 2010). Meanwhile, DOX mole fraction solubility at 298.15 K was reported at 0.21 and 1.98 for pure H_2O and MeOH, respectively (Shen et al., 2019; Shen et al., 2020). (See Table 1.)

3.3. Mass analysis

Spectral analysis based on TIC confirms the identity of the compounds tested, as they can be compared and matched with other mass spectra reported in the literature for STM and DOX. For example, van Bruijnsvoort et al. (2004) reported for STM obtained with and LC-MS/MS and ESI$^+$ a spectra with main signals at 582 ([M + H]$^+$), 407 ([$C_{14}H_{25}N_6O_8^{\bullet}$ + 2H]$^+$), 263 ([$C_8H_{17}N_6O_4^{\bullet}$ + 2H]$^+$), 246 ([$C_8H_{17}N_6O_3^{\bullet}$ + H]$^+$), 221, and 176 ($C_7H_{14}NO_4^{\bullet}$) *m/z*; all signals that can be found in our analysis (see Fig. 1C). An analogous analysis can be done for doxycycline (see Fig. 1D) with two main signals, 445 ([M + H]$^+$) and 428 (loss of an amino group) *m/z* [see for example, (Bouslimani et al., 2014)]. Each TIC was used to identify the molecular ion signal (Fig. 1C, D). Thereafter, SIM was used to corroborate each compound identity, remove interferences and improve sensitivity (Fig. 1E, F).

3.4. Method performance and validation parameters

The method was validated according to performance parameters dictated by international guidelines (Borman and Elder, 2018; Raposo and Ibelli-Blanco, 2020; US FDA, 2015). Approximately two mg of STM and DOX were placed in a 10 mL volumetric flask and diluted with the appropriate solvent (i.e., H_2O for STM and MeOH for DOX) to prepare a stock solution of 200 μg mL^{-1}. After that, by combining aliquots of both compounds and a subsequent ten-fold dilution (matching the same proportion of solvents used for antimicrobial extraction in tissue; see Section 2.4), a working solution of 20 μg mL^{-1} was obtained. The injection of 0.625, 1.25, 3, 6, 9, 12, and 15 μL from the aforementioned working solution allows the construction of eight-point calibration curves ranging from 0.625 to 15 μg mL^{-1} (Table 2, Fig. 2A, B). An excellent linear association among variables (area vs. concentration) was observed as determined by coefficients of determination (i.e., $r^2 >$ 0.90, Table 2). Working concentrations were selected considering the therapeutic dosage for STM and DOX typically administered to treat Brucellosis (e.g., 900 mg SID (15 mg kg^{-1} bw) for 7–14 days intramuscularly and 100 mg BID (5 mg kg^{-1} bw) for 45 days orally, respectively (Corbel, 2006; Solera et al., 1995). Likewise, a standard containing exactly 1.00 μg mL^{-1} was used to obtain each drug's response factors (Area$_{std}$/Concentration$_{std}$).

Table 1
Optimized detection conditions for both antimicrobials tested.

Antimicrobial	Retention time (t_R), min	Cone Voltage/ Fragmentor, V	Molecular ion, *m/z*
STM	2.412 ± 0.151	200	[M + H]$^+$, 582.3; [M + Na]$^+$, 614.3; [M + K]$^+$, 620.3
DOX	14.288 ± 0.107	120	[M + H]$^+$, 445.1

Table 2
Parameters obtained for the method as per linearity.

Antimicrobial	Equation	R	R^2	Standard error of estimation
STM	$y = (1.698 \pm 0.067)x + (0.317 \pm 0.519)$	0.9953	0.9907	0.9396
DOX	$y = (1.317 \pm 0.037)x + (1.413 \pm 0.297)$	0.9976	0.9945	0.5706

Data for column performance was extracted from an average of $n = 3$ injections of the 1.00 μg mL^{-1} standard in conditions of reproducibility (Table 3). Altogether, these values imply adequate column efficiency and symmetric signals or peaks during elution (i.e., no significant tailing or fronting). As only two signals are separated with almost 12 min apart, $\alpha_s > 5$ and $R_s >> 2$ (Fig. 1A, B). Theoretical plates were calculated using the width of the peak at the half-height [i.e., $N = 5.54 \cdot (t_R/w_{0.5})^2$].

Matrix-matched calibration curves including blank samples were constructed for each type of sample to be tested to assess the limits of detection and quantitation, calculated as 3.3 and 10 times the signal-to-noise ratio, respectively (Table 4, Fig. 3A, B). Experiments corroborated these limits to extinction. Final limits ranged from 39.54 ng mL^{-1}/65.90 to 494.27 ng g^{-1}and 21.05 ng mL^{-1}/33.34 to 263.07 ng g^{-1} for STM and DOX, respectively (Table 4). As the amount of material available in bone marrow was limited, sensitivity was still high for this matrix with detection for STM achieving values of 494.27 μg g^{-1} (Table 4). Furthermore, as the extraction solvent was also kept in the microliter range (i.e., 500 μL total), acceptable sensitivity was attained despite avoiding clean up and concentration steps (Table 4).

In the form of precision and reproducibility, repeatability was within accepted values [i.e., 7.5–11%, (Van Breemen et al., 2018)]. Again, the simplicity of the extraction method demonstrated a little more matrix effects, as seen in the sample blanks (mostly region 23–30 min, Figs. 1A, B, 3A, and 4A, B), but ensured high reproducibility and accuracy (Table 5, Fig. 3B, 4A, B, 5A, B). The matrix that exhibited more consistence in terms of variability, was plasma (0.46 and 0.84%RSD, Table 5, Fig. 4B). Analogously, recoveries were acceptable for a method working range of μg g^{-1} [i.e., 75–120%, (Van Breemen et al., 2018)]. Values ranged from 75.23 ± 1.93 (for bone marrow) to 101.33 ± 1.23% (for liver) (Table 5, (Fig. 3B, 5A, B).

As sample preparation was quite simple and repeatability and accuracy were within acceptable values (see above), an internal standard may not add any benefit (Bergeron et al., 2009). Additionally, the suppliers for stable isotope analogs of doxycycline and streptomycin are few, and those available cannot provide a labeled standard with the purity required (Bergeron et al., 2009). Finally, using other (non-deuterated) aminoglycoside and tetracycline congeners as internal standards is not advisable. These also have veterinary benefits and may exhibit different behaviors during extraction and chromatography (van Holthoon et al., 2010).

3.5. Real sample application

The high incidence of relapses in Brucellosis in humans (even under the recommended antibiotic regimen) raises questions about the dosages of administration. More specifically, if the current regimen can reach complex access sites such as bone marrow, which bacteria use as a long-term niche (Gutierrez-Jiménez et al., 2018; Gutierrez-Jiménez et al., 2019).

The approach employed in this study permitted extracting (and measuring) STM and DOX from complex matrices such as mice tissue and plasma rapidly and effectively, without loss of the analytical accuracy and successfully minimizing matrix effects. Furthermore, we have shown that using a mouse model, the recovery and quantification of STM and DOX in plasma, liver, and bone marrow are observed after 12 h of administering the three different doses for each antibiotic (Fig. 6).

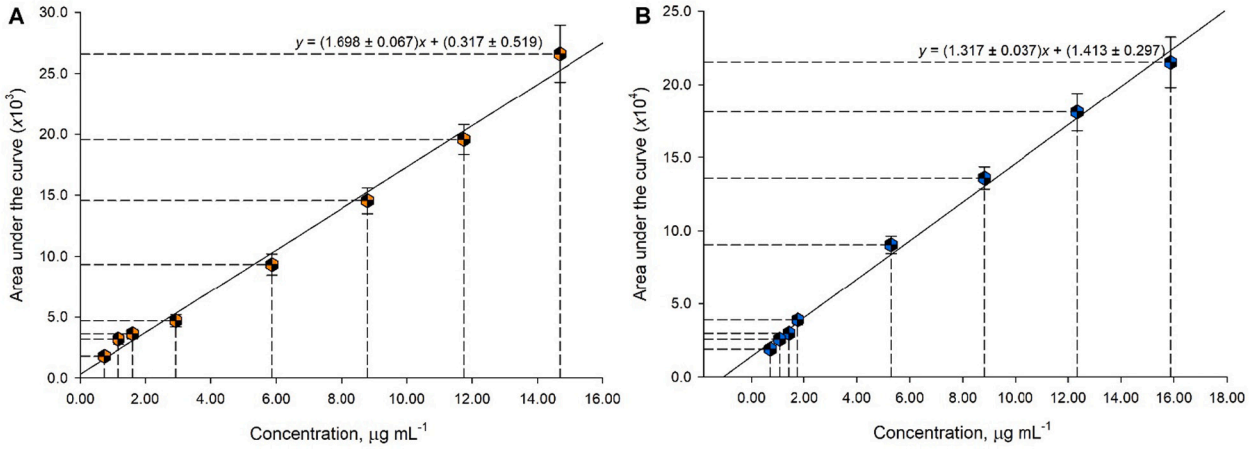

Fig. 2. Standard calibration curves for A. STM and B. DOX. The resulting curve results from five replicates of each, with error bars as $SE_{x/y}$.

Table 3
Chromatography performance parameters for the separation of the antimicrobials.

Parameter/Antimicrobial	Theoretical plates (*N*)	Capacity factor (*k'*)	Selectivity (α_s)	Resolution (R_s)	Asymmetry factor (A_s)	Tailing factor (T_f)
STM	2164	3.28	–	–	1.13	0.07
DOX	6454	24.88	7.58	22.58	1.49	0.45

Table 4
Sensitivity parameters of the proposed methods for both antimicrobials tested.

Compound/Matrix	Instrumental	Liver	Kidney	Spleen	Bone marrow	Plasma
	ng mL^{-1}	*ng g*$^{-1}$				*ng mL*$^{-1}$
Limits of detection						
STM	11.86	65.90	62.65	73.45	494.27	39.54
DOX	6.31	35.08	33.34	37.67	263.07	21.05
Limits of quantitation						
STM		199.70	189.86	222.56	1497.79	119.82
DOX		106.29	101.03	114.14	797.19	63.78

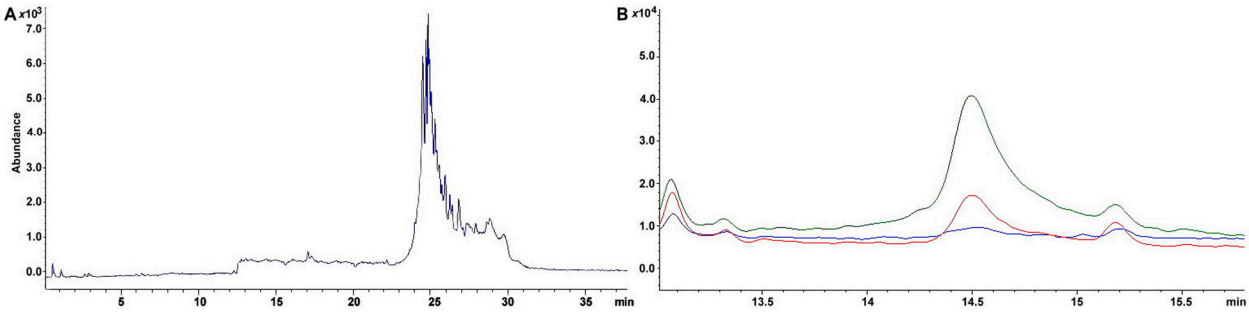

Fig. 3. Chromatogram for A. Matrix blank for liver samples B. Spiked bone marrow sample. Blue line: Matrix blank, red line: standard 3.2 µg mL^{-1} DOX, green line: recovery experiment for 6.5 µg g^{-1} DOX. (For interpretation of the references to colour in this figure legend, the reader is referred to the web version of this article.)

Overall, we demonstrated a significant percentage of tissue allocation of the antimicrobial, even at the lowest concentrations administered (Fig. 7B-E). Besides, the result obtained in our experimental model shows a dose-response relationship between the fraction administered and that recovered. Most results showed the higher doses correlated with the highest allocation percentages in the tissue. However, the 20 and 10 mg kg^{-1} doses for STM showed similar allocation percentages for all tissues tested (Fig. 7A- C).

On the other hand, the low STM allocation in the liver compared to plasma and bone marrow (ca. 10/20-fold, Fig. 7C) could be explained considering the high polarity of the antimicrobial molecule. Its high partition in water (log *P* -7.7) allows for little to no hepatic metabolism. Analogously, for DOX in the liver, the lowest administration dose (i.e., 50 mg kg^{-1}) resulted in almost no allocation of the antimicrobial in this tissue. This result could be related to a preferred renal and gastrointestinal route of metabolism at low doses (Agwuh and MacGowan, 2006) and (relative) hydrophobic character of the molecule (log *P* between −1.90 and 0.63, Fig. 7F).

Finally, though internalization in some tissues seems to be dose-dependent, concentrations must be closely monitored to avoid drug

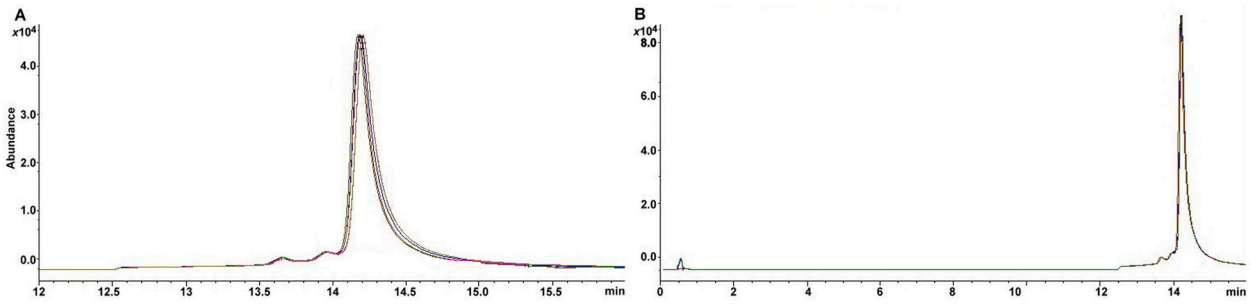

Fig. 4. Superimposed injections to reflect method repeatability for DOX A. Five individual spiked liver samples at 6.25 μg g^{-1} B. Three individual spiked plasma samples at 12.5 μg mL^{-1}.

Table 5
Recovery example obtained for liver, mean accuracy, and repeatability obtained for all the matrices tested.

Liver									
				STM			DOX		
				Area under the curve					
Standard				$129192_{16\ mgkg^{-1}}$			$833366_{3\ mgkg^{-1}}$		
Spiked liver				279,569			954,090		
Sample w/o spiking				1575.79			43,454.8		
Experimental/Obtained				277,993.21			910,635.2		
Recovery, %				99.43			95.44		
Liver		*Kidney*		*Spleen*		*Bone marrow*		*Plasma*	
STM	*DOX*	*STM*	*DOX*	*STM*	*DOX*	*STM*	*DOX*	*STM*	*DOX*
Recovery per matrix, %[a]									
101.33 ± 1.23	95.73 ± 1.05	96.76 ± 0.99	98.80 ± 1.13	88.33 ± 2.23	85.09 ± 1.87	75.23 ± 1.93	79.93 ± 0.93	100.03 ± 0.23	101.13 ± 0.78
Intraday repeatability, %RSD									
1.34	2.51	1.68	1.01	1.89	2.00	4.82	4.89	0.58	0.46
Interday repeatability, %RSD									
2.34	3.51	1.68	2.01	1.44	2.11	11.20	10.87	0.97	0.87

[a] Recoveries expressed as median values ± SE_x.

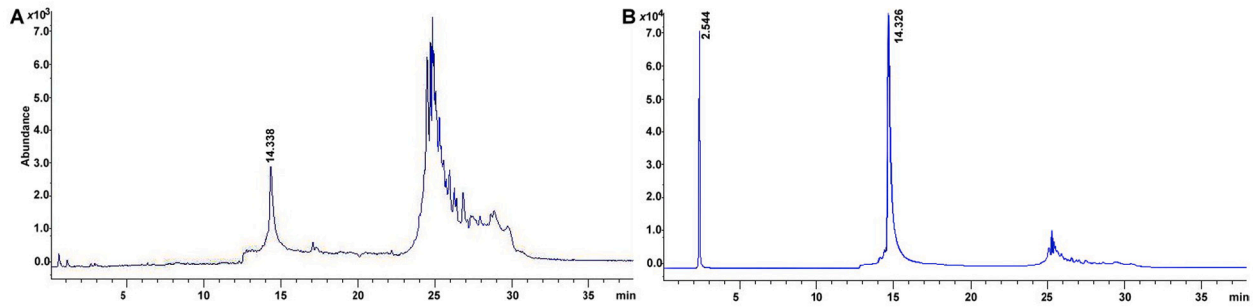

Fig. 5. Example of a recovery experiment in an organ A. Liver sample after dosing with DOX B. Spiked liver sample with 16 and 3 μg g^{-1} STM and DOX, respectively.

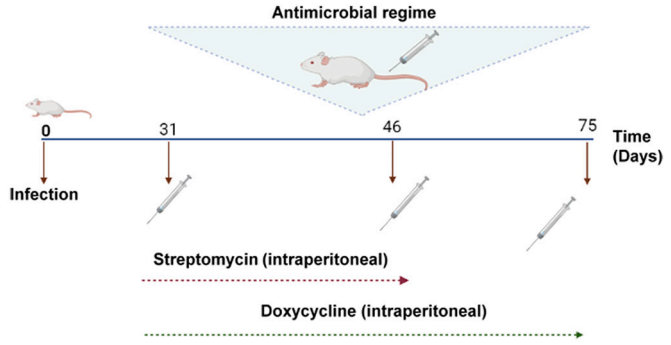

Fig. 6. Therapeutic model proposed for murine models after *Brucella* infection using double antimicrobial treatment with STM and DOX at nominal concentrations ranging from 10 to 40 and from 50 to 200 mg kg^{-1}.

side effects. For example, STM is a narrow therapeutic index drug; exceeding recommended dosages can generate oto- and nephrotoxicity (Klis et al., 2014). DOX cannot exceed 300 mg per day as dermatological, skeletal, and gastrointestinal side effects occur. A maximum dosage of 2.2 mg kg^{-1} per day is permitted when benefits outweigh the risks (Holmes and Charles, 2009).

4. Conclusions

Simple sample pretreatment and the simultaneous analysis of both antimicrobials, aided by the mass detector, allowed us to monitor the two different therapeutic drugs easily and generate a high throughput method. Under different chromatographic conditions, one might need two different derivatization methods or the use of two separate detectors. The proposed approach was fast, reliable, accurate, and easy to execute as it has minimal sample pretreatment (i.e., based on freeze-drying, deproteinization and centrifugation alone). Hence, the

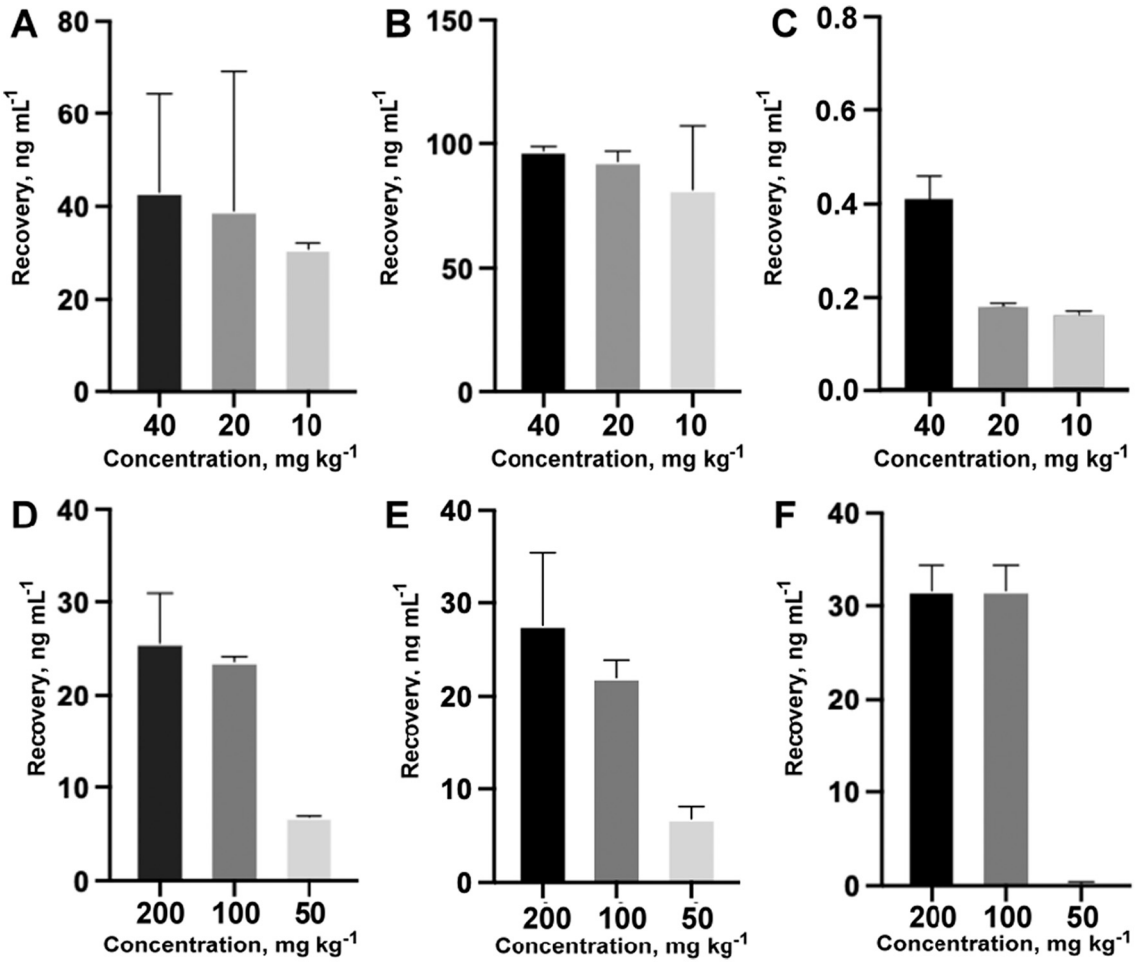

Fig. 7. Allocation levels of antibiotics after their therapeutic administration on mice for STM in A. plasma, B. bone marrow, and C. liver and DOX in D. plasma, E. bone marrow, and F. liver.

developed and validated method meets its intended purpose's requirements and can be further exploited in metabolism studies of antimicrobials involving parent compound depletion or accumulation in targeted animal tissue. Experimental extraction of antimicrobial in actual murine tissue demonstrated selective deposition for STM in plasma and bone marrow and very poor allocation in the liver. DOX apportionment in all three matrices tested seems to be alike. The data above justify a further examination of tissue distribution of antimicrobials, in such models, used during Brucellosis therapy.

Ethics

All procedures regarding animals were performed in accordance and consent of the "Institutional Committee for the Care and Use of Animals of the University of Costa Rica (CICUA-036-2021)," the "Guide for the care and use of laboratory animals" [33], and in accordance with the corresponding "Animal Welfare Law 9458 of Costa Rica."

'Authors' contribution

All authors contributed equally to this work.

Declaration of Competing Interest

The authors declare that they have no known competing financial interests or personal relationships that could have appeared to influence the work reported in this paper.

Acknowledgements

The authors would like to thank the Costa Rican National Council of Provosts who partially funded this research (grant FEES-CONARE, 803-C2-651/SIA0492-21)(https://www.conare.ac.cr) and fellowship support for Eugenia Sancho from the Master's Programme in Microbiology, University of Costa Rica.

References

Abo El-Ela, F.I., Hussein, K.H., El-Banna, H.A., Gamal, A., Rouby, S., Menshawy, A.M.S., El-Nahass, E.S., Anwar, S., Zeinhom, M.M.A., Salem, H.F., Al-Sayed, M.A.Y., El-Newery, H.A., Shokier, K.A.M., El-Nesr, K.A., Hosein, H.I., 2020. Treatment of brucellosis in Guinea pigs via a combination of engineered novel pH-responsive curcumin Niosome hydrogel and doxycycline-loaded chitosan-sodium alginate nanoparticles: an *in vitro* and *in vivo* study. AAPS Pharm. Sci. Tech. 21 (8), 326.

Agwuh, K.N., MacGowan, A., 2006. Pharmacokinetics and pharmacodynamics of the tetracyclines including glycylcyclines. J. Antimicrob. Chemother. 58 (2), 256–265.

Alavi, S.M., Alavi, L., 2013. Treatment of brucellosis: a systematic review of studies in recent twenty years. Casp. J. Int. Med. 4 (2), 636–641.

Alkhzem, A.H., Woodman, T.J., Blagbrough, I.S., 2020. Individual pK_a values of tobramycin, kanamycin B, amikacin, sisomicin, and netilmicin determined by multinuclear NMR spectroscopy. ACS Omega 5 (33), 21094–21103.

Alp, E., Kermal Koc, R., Candan Durak, A., Yildiz, O., Aygen, B., Sumerkan, B., Doganay, M., 2006. Doxycycline plus streptomycin versus ciprofloxacin plus rifampicin in spinal brucellosis. BMC Infect. Dis. 6, 72.

Araby, E., Nada, H.G., Abou El-Nour, S.A., Hammad, A., 2020. Detection of tetracycline and streptomycin in beef tissues using Charm II, isolation of relevant resistant bacteria and control their resistance by gamma radiation. BMC Microbiol. 20 (1), 186.

Barquero-Calvo, E., Chacón-Diaz, C., Chaves-Olarte, E., Moreno, E., 2013. Bacterial counts in spleen. Bio-protocol 3 (21), 1–6.

Bergeron, A., Furtado, M., Garofolo, F., 2009. Importance of using highly pure internal standards for successful liquid chromatography/tandem mass spectrometric bioanalytical assays. Rapid Commun. Mass Spectrom. 23 (9), 1287–1297.
Bohm, D.A., Stachel, C.S., Gowik, P., 2012. Confirmatory method for the determination of streptomycin and dihydrostreptomycin in honey by LC-MS/MS. Food Addit. Contam. 29 (2), 189–196.
Borman, P., Elder, D., 2018. In: Teasdale, A., Elder, D., Nims, R.W. (Eds.), Q2(R1) Validation of Analytical Procedures In ICH Quality Guidelines: An implementation Guide. John Wiley & Sons, Inc, Hoboken, NJ, USA.
Bouslimani, A., Sánchez, L.M., Garg, N., Dorrestein, P.C., 2014. Mass spectrometry of natural products: current, emerging and future technologies. Nat. Prod. Rep. 31 (6), 718–729.
Boxer, G.E., Jelinek, V.C., 1947. A chemical method for the determination of streptomycin in blood and spinal fluid. J. Biol. Chem. 170, 491–500.
Cazorla-Reyes, R., Romero-González, R., Garrido Frenich, A., Rodríguez Maresca, M.A., Martínez Vidal, J.L., 2014. Simultaneous analysis of antibiotics in biological samples by ultra high performance liquid chromatography-tandem mass spectrometry. J. Pharm. Biomed. Anal. 89, 203–212.
Chaitanya Krishna, A., Sathiyaraj, M., Saravanan, R.S., Chelladurai, R., Vignesh, R., 2012. A novel and rapid method to determine doxycycline in human plasma by liquid chromatography tandem mass spectrometry. Indian J. Pharm. Sci. 74 (6), 541–548.
Cooper, K.M., Mulder, P.P.J., van Rhijn, J.A., Kovacsics, L., McCracken, R.J., Young, P.B., Kennedy, D.G., 2005. Depletion of four nitrofuran antibiotics and their tissue-bound metabolites in porcine tissues and determination using LC-MS/MS and HPLC-UV. Food Addit. Contam. 22 (5), 406–414.
Corbel, M.J.J., 2006. Food and Agriculture Organization of the United Nations, World Health Organization & World Organisation for Animal Health. Brucellosis in Humans and Animals. World Health Organization. https://apps.who.int/iris/handle/10665/43597.
Do, J.-A., Lee, M.-Y., Cho, Y.-J., Chang, M.-I., Hong, J.-H., Oh, J.-H., 2015. Determination of streptomycin in kiwifruit samples using LC-ESI-MS/MS. Anal. Sci. Technol. 28 (4), 299–307.
Gadja, A., Posyniak, A., Tomczyk, G., 2014. LC-MS/MS analysis of doxycycline residues in chicken tissues after oral administration. Bull. Vet. Inst. Pulawy 58 (4), 573–579.
Gengerbacher, M., Zimmerman, M.D., Sarathy, J.P., Kaya, F., Wang, H., Mina, M., Carter, C., Hossen, A., Su, H., Trujillo, C., Ehrt, S., Schnappinger, D., Dartois, V., 2020. Tissue distribution of doxycycline in animal models of tuberculosis. Antimicrob. Agents Chemother. 64 (5) e02479–19.
Gerhardt, G.C., Salisbury, C.D., MacNeil, J.D., 1994. Determination of streptomycin and dihydrostreptomycin in animal tissues by on-line sample enrichment liquid chromatography. J. AOAC Int. 77 (2), 334–337.
Giusepponi, D., Paoletti, F., Barola, C., Moretti, S., Saluti, G., Ianni, F., Sardella, R., Galarini, R., 2019. Transfer of a multiclass method for over 60 antibiotics in food from high resolution to low resolution mass spectrometry. Molecules 24 (16), 2935.
Granados-Chinchilla, F., Rodríguez, C., 2017. Tetracyclines in food and feedingstuffs: from regulation to analytical methods, bacterial resistance, and environmental and health implications. J. Anal. Meth. Chem. 2017, 1–24. Article ID 1315497.
Grilló, M.J., Blasco, J.M., Gorvel, J.P., Moriyón, I., Moreno, E., 2012. What have we learned from Brucellosis in the mouse model? Vet. Res. 13 (1), 29.
Gutierrez-Jiménez, C., Hysenaj, L., Alfaro-Alarcón, A., Mora-Cartín, R., Arce-Grovel, V., Moreno, E., Gorvel, J.P., Barquero-Calvo, E., 2018. Persistence of *Brucella abortus* in the bone marrow of infected mice. J Immunol Res 2018 (69), 5370414.
Gutierrez-Jiménez, C., Mora-Cartín, R., Altamirano-Silva, P., Chacón-Díaz, C., Chaves-Olarte, E., Moreno, E., Barquero-Calvo, E., 2019. Neutrophils as Trojan Horse vehicles for Brucella abortus macrophage infection. Front. Immunol. 10. Article 1012.
Harrison, E.R., Posada, R., 2018. Brucellosis. Pediatr. Rev. 39 (4), 222–224.
Holmes, N.E., Charles, P.G.P., 2009. Safety and efficacy review of doxycycline. Clin. Med. Insight Ther. 1, 471–482.
Hormazábal, V., Østensvik, Ø., 2009. Determination of streptomycin and dihydrostrptomycin in milk and meat by liquid chromatography – mass spectrometry. J. Liquid Chrom. Rel. Technol. 32 (18), 2756–2764.
Hušek, P., Švagera, Z., Hanzílová, D., Šimek, P., 2012. Survey of several methods deproteinizing human plasma before and within the chloroformate-mediated treatment of amino/carboxylic acids quantitated by gas chromatography. J. Pharm. Biomed. Anal. 67-68, 159–162.
Institute for Laboratory Animal Research (ILAR) of the National Research Council Animal Care and Use Program/Veterinary Care, 2011. In Guide for the Care and Use of Laboratory Animals. National Academies Press, Washington DC, USA.
Jelinek, V.C., Boxer, G.E., 1948. A chemical determination of streptomycin in body tissues and urine. J. Biol. Chem. 175 (1), 367–375.
Kirst, H.A., Allen, N.E., 2007. In: Taylor, J.B., Triggle, D.J. (Eds.), Aminoglycosides Antibiotics in Comprehensive Medicinal Chemistry II. Elsevier Science, Amsterdam, Netherlands.
Klis, S., Stienstra, Y., Philips, R.O., Abass, K.M., Tuah, W., van der Werf, T.S., 2014. Long term streptomycin toxicity in the treatment of Buruli ulcer: follow-up of participants in the BURULICO drug trial. PLoS Negl. Trop. Dis. 8, e2739.
Krause, K.M., Serio, A.W., Kane, T.R., Connolly, L.E., 2016. In: Silver, L.L., Bush, K. (Eds.), Aminoglycosides: An Overview in Additional Perspectives on Antibiotics and Antibiotics Resistance. Cold Spring Harbor Laboratory Press, NY, USA.
Mallet, C.R., Lu, Z., Mazzeo, J.R., 2004. A study on ion suppression effects in electrospray ionization from mobile phase additives and solid-phase extracts. Rapid Commun. Mass Spectrom. 18 (1), 49–58.
Markley, J.L., Wencewicz, T.A., 2018. Tetracycline-inactivating enzymes. Front. Microbiol. 9, 1058.
Mestorino, N., Zeinsteger, P., Buchamer, A., Buldain, D., Aliverti, F., Marchetti, L., 2018. Tissue depletion of doxycycline after its oral administration in food producing chicken for fattening. Int. J. Avian Wildlife Biol. 3 (3), 245–250.
Mitchison, D.A., Spicer, C.C., 1949. A method of estimating streptomycin in serum and other body fluids by diffusion through agar enclosed in glass tubes. Microbiology 3 (2), 184–203.
Mojica, E.-R.E., Nguyen, E., Rozov, M., Bright, F.V., 2014. pH-dependent spectroscopy of tetracycline and its analogs. J. Fluoresc. 24 (4), 1183–1198.
Okayama, A., Kitada, Y., Aoki, Y., Umesako, S., Ono, H., Nishi, Y., 1988. Fluorescence HPLC determination of streptomycin in meat using ninhydrin as a post-column labeling agent. J-STAGE 37 (5), 221–224.
Pappas, G., Papadimitriou, P., Akritidis, N., Christou, L., Tsianos, E.V., 2006. The new global map of human Brucellosis. Lancet Infect. Dis. 6 (2), 91–99.
Ramirez Raneses, J., Ellison, A.L., Liu, B., Davis, K.M., 2020. Subpopulation of stressed *Y. pseudotuberculosis* preferenatially survive doxycycline treatment within host tissue. Mbio 11 (4), e00901–e00920.
Raposo, F., Ibelli-Blanco, C., 2020. Performance parameters for analytical method validation: controversies and discrepancies among numerous guidelines. TrAC Trends Anal. Chem. 129, 115913.
Samanidou, V., Bitas, D., Charitonos, S., Papadoyannis, I., 2016. On the extraction of antibiotics from shrimps prior to chromatographic analysis. Separations 3 (1), 8.
Selvadural, M., Mayyanathan, S.N., Rajan, S., Padmanaban, G., Suresh, B., 2010. Determination of doxycycline in human plasma by liquid chromatography-mass spectrometry after liquid-liquid extraction and its application in human pharmacokinetics studies. J. Bioequiv. Availab. 2 (4), 093.
Shen, Y., Liu, W., Bao, Z., 2019. Solubility measurement and thermodynamic modeling of doxycycline hyclate two binary solvent systems at 276.96-323.75 K. J. Mol. Liq. 289, 111138.
Shen, Y., Liu, W., Sun, C., Shi, P., 2020. Solubility measurement and correlation of doxycycline hyclate in 10 pure solvents and mixtures solvents at 278.15−323.15 K. J. Chem. Eng. Data 65 (5), 2774–2783.
Silva, T.M., Costa, E.A., Paixão, T.A., Tsolis, R.M., Santos, R.L., 2011. Laboratory animal models for Brucellosis research. J. Biomed. Biotechnol. 2011, 518323.
Solera, J., 2010. Update on Brucellosis: therapeutic challenges. Int. J. Antimicrob. Agents 36 (Suppl. 1), S18–S20.
Solera, J., Rodríguez-Zapata, M., Geijo, P., Largo, J., Paulino, J., Sáez, L., Martínez-Alfaro, E., Sánchez, L., Sepulveda, M.-A., Ruiz-Ribó, M.-D., GECMEI Group, 1995. Doxycycline-rifampin versus doxycycline-streptomycin in treatment of human brucellosis due to *Brucella melitensis*. Anitmicrob. Agents Chemother. 39 (9), 2061–2067.
Ujváry, I., 2010. In: Krieger, R.I., Krieger, W.C. (Eds.), Pest Control Agents from Natural Products in Hayes' Handbook of Pesticide Toxicology. Academic Press, Inc, Cambridge, MA, USA.
US FDA, 2015. Analytical Procedures and Methods Validation for Drugs and Biologics, Guidance for Industry. Available from, CDER. Last Accessed, 11th December 2020. https://www.fda.gov/downloads/drugs/guidances/ucm386366.pdf.
Van Breemen, R., Bzhelyansky, R., Es-Safi, N.E., Jennens, M., Johnson, H.E., Krepich, S., Kuszak, A., Monagas, M., Reif, K., Rimmer, C.A., Solyom, A.M., Stewart, J., Szpylka, J., You, H., Young, K., Zhao, H., Zielinski, G., 2018. *Standard method performance requirements* (SMPRs®) 2018.004: determination of *trans* resveratrol in dietary supplements and dietary ingredients. J. AOAC Int. 101 (4), 1254–1255.
van Bruijnsvoort, M., Ottink, S.J.M., Jonker, K.M., de Boer, E., 2004. Determination of streptomycin and dihydrostreptomycin in milk and honey by liquid chromatography with tandem mass spectrometry. J. Chrom. A. 1058 (1–2), 137–142.
van Holthoon, F., Mulder, P.P.J., van Bennekom, E.O., Heskamp, H., Zuidema, T., van Rhijn, H.A., 2010. Quantitative analysis of penicillins in porcine tissues, milk and animal feed using derivatisation with piperidine and stable isotope dilution liquid chromatography tandem mass spectrometry. Anal. Bioanal. Chem. 396 (8), 3027–3040.
Vardanyan, R.S., Hruby, V.J., 2006. In: Vardanyan, R.S., Hruby, V.J. (Eds.), Antibiotics in Synthesis of Essential Drugs. Elsevier Science, Amsterdam, Netherlands.
Whatmore, A.M., Foster, J.T., 2021. Emerging diversity and ongoing expansion of the genus *Brucella*. Infect. Genet. Evol. 92, 104865.
Xu, N., Dong, J., Zhou, W., Liu, Y., Ai, X., 2019. Determination of doxycycline, −4epidoxycycline, and 6-epidoxycycline in aquatic animal muscle tissue by an optimized extraction protocol and ultra-performance liquid chromatography with ultraviolet detection. Anal. Lett. 52 (3), 452–464.
Xu, N., Li, M., Ai, X., Lin, Z., 2021. Determination of pharmacokinetics and pharmacokinetic-pharmacodinamic parameters of doxycycline against *Edwardsiella ictaluri* in yellow catfish. Antibiotics 10 (3), 329.
Zhang, X., Wang, J., Wu, Q., Li, L., Wang, Y., Yang, H., 2019. Determination of kanamycin by high performance liquid chromatography. Molecules 24 (10), 1902.